Journal of Molecular Spectroscopy 387 (2022) 111666

Contents lists available at ScienceDirect

Journal of Molecular Spectroscopy

journal homepage: www.elsevier.com/locate/yjmsp

Rotational and hyperfine analysis of the $D^2\Pi_{1/2} - X^2\Delta_{3/2}$ (0,0) band of TaO

Kevin A. Tovar, Thomas D. Varberg *

Department of Chemistry, Macalester College, 1600 Grand Ave., St. Paul, MN 55105, USA

ARTICLE INFO

Keywords:
Tantalum oxide
Electronic spectrum
Rotational
Hyperfine

ABSTRACT

The $D^2\Pi_{1/2} - X^2\Delta_{3/2}$ transition of TaO has been analyzed for the first time by recording a laser excitation spectrum of its (0,0) band, which lies near 696 nm. This band was first observed many years ago by Cheetham and Barrow (*Trans. Faraday Soc.* 63 (1967) 1835–1845), who did not undertake an analysis due to the dense rotational structure. The spectrum displays broad hyperfine structure arising from the ^{181}Ta nucleus that is well resolved at the Doppler-limited resolution of the experiment. The data were fitted using an effective Hamiltonian expressed in a Hund's case (c) basis, confirming the upper state symmetry as $^2\Pi_{1/2}$ and yielding an accurate set of molecular constants describing its rotational and hyperfine structure.

1. Introduction

The electronic spectra of transition metal monoxides and monosulfides are relevant to astronomy. For example, TiO [1] and VO [2] produce prominent bands in the spectra of M type stars that are used in temperature profiling studies. The molecules TiS, ZrO, YO, and ZrS have also been seen in cold stars [3], and the title molecule, TaO, has been tentatively identified in the atmosphere of the S star *R Cyg* [4]. The 5d transition metal diatomic molecules are also of interest to researchers seeking to measure the electric dipole moment of the electron, and the TaO^+ cation has been proposed as a candidate for such studies [5].

The electronic spectrum of TaO in the gas phase was first recorded in emission in 1955 by Premaswarup [6], who identified three bands between 370 and 430 nm. Premaswarup and Barrow [7] followed this work with a revised analysis of the three bands, all of which involve a common lower level assigned as a $^2\Delta_{3/2}$ state. A decade later, Weltner and McLeod [8] recorded the absorption spectrum of tantalum oxide isolated in solid argon and neon matrices. Sixteen different electronic transitions spanning the wavelength range 843 to 336 nm were found, including the three previously identified gas-phase transitions, from which it was concluded that the lower $^2\Delta_{3/2}$ state is the ground state of the molecule. One of these transitions was a D–X (0,0) band at 14,395 cm^{-1}, with ^{18}O isotopic substitution demonstrating the upper state vibrational assignment to be $v' = 0$. The matrix work prompted Cheetham and Barrow [9] to record the gas-phase emission spectrum again over a wide wavelength range, leading to the identification of 19 different excited electronic states in the near-infrared, visible and ultraviolet regions. These authors reported the wavenumber of the D–X (0,0) transition as 14,370 cm^{-1} but did not undertake a rotational analysis due to the significant line broadening seen at high resolution. They speculated this broadening arises from unresolved hyperfine structure and tentatively assigned the D state to have $\Omega = 1/2$. To clarify the symmetries of all the known upper states, Brittain *et al.* [10] recorded magnetic circular dichroism (MCD) spectra of TaO in a solid argon matrix. Based on the phase of the observed MCD signal, the D state was assigned to be of $^2\Pi_{1/2}$ character.

More recently, several new electronic transitions in the gas-phase molecule have been found in emission using Fourier transform spectrometry by Al-Khalili *et al.* [11] and Ram and Bernath [12,13]. Some of these transitions involve a lower level that is not the ground state, assigned to be either a $^2\Sigma$ [11] or $^2\Pi$ state [13]. Accurate computational studies of the various excited electronic states of TaO would be of obvious help here, but we are aware of *ab initio* calculations on only the $X^2\Delta$ and low-lying $a^4\Sigma^-$ states [14–17]. The photoelectron spectrum of the TaO^- anion has been recorded by Zheng *et al.* [18]. Analysis of the photodetachment transitions to the neutral product confirmed the energies of several previously identified doublet states of TaO and for the first time experimentally located the $a^4\Sigma^-$ state to be 0.71(6) eV (5730 ± 480 cm^{-1}) above the ground state.

Our interest in TaO was stimulated both by a desire to analyze the hyperfine structure of some of its transitions, in the hope of illuminating aspects of its electronic structure and chemical bonding, and to rotationally analyze bands that remain unassigned. We have previously reported our results for the $B^2\Phi_{5/2} - X^2\Delta_{3/2}$, $C^2\Delta_{3/2} - X^2\Delta_{3/2}$, and

* Corresponding author.
E-mail addresses: ktovar@macalester.edu (K.A. Tovar), varberg@macalester.edu (T.D. Varberg).

https://doi.org/10.1016/j.jms.2022.111666
Received 6 May 2022; Received in revised form 12 June 2022; Accepted 13 June 2022
Available online 20 June 2022

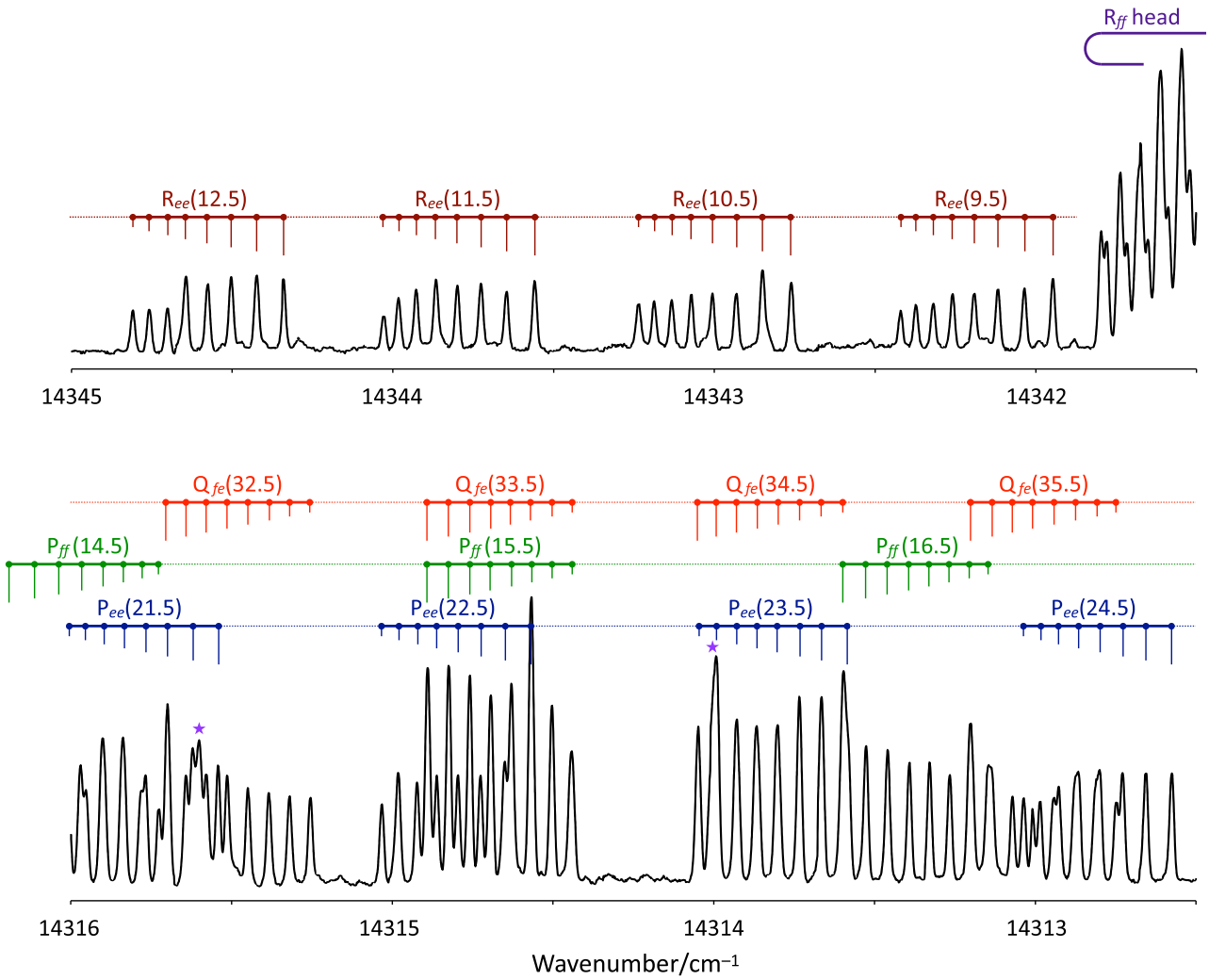

Fig. 1. Laser excitation spectrum of the TaO $D^2\Pi_{1/2} - X^2\Delta_{3/2}$ (0,0) band, with the upper and lower traces displaying separate 3.5 cm^{-1} wide portions. Each rotational transition has eight ^{181}Ta hyperfine components that are marked by vertical lines, for which $\Delta F = \Delta J$. The longest line represents the maximum F component, which lies to lowest wavenumber for rotational transitions involving the upper state e parity component, while for the f parity, this hyperfine pattern is reversed. The stars on two blended lines in the lower trace mark overlapping P lines from the TaO $C^2\Delta_{3/2} - X^2\Delta_{3/2}$ (3,2) band.

$E^2\Pi_{1/2} - X^2\Delta_{3/2}$ transitions [19,20]. Here, we present a rotational and hyperfine analysis of the as yet unassigned D–X transition. Our rotational analysis demonstrates conclusively that the upper state is indeed $^2\Pi_{1/2}$, in agreement with the MCD results [10]. While the spectrum is too congested to permit an identification of the first lines in the six rotational branches, unambiguous evidence for this upper state assignment comes in several other forms. The presence of a strong (Λ-doubled) Q branch implies a perpendicular transition, which means the D state is either $^2\Pi_{1/2}$ or $^2\Phi_{5/2}$, and the large Λ-doubling eliminates the possibility of $^2\Phi_{5/2}$, for which little or no resolvable splitting would be expected. The $B^2\Phi_{5/2}$ and $C^2\Delta_{3/2}$ states of TaO, for example, display no Λ-doubling even at sub-Doppler resolution [19]. Furthermore, the hyperfine structure of the D–X band is dominated by the parity-dependent Λ-doubling term described by the parameter d in the upper state, which is a term in the magnetic dipole Hamiltonian that exists only in Π states.

2. Experiment

Gaseous TaO molecules were generated using a hollow cathode sputtering source, in which a 32-mA DC electric discharge was maintained in argon, with a small amount of hydrogen added to stabilize the discharge, which improves the signal-to-noise ratio. It is likely that the oxygen required to make TaO comes from the surface of the cathode itself, since the addition of a small amount of O_2 or N_2O to the flowing gas mixture *decreases* the strength of the TaO signal. The gas mixture flowed through a 1-mm hole in a 6-mm diameter, 12-mm long tantalum cathode. The plasma was expanded through a 3-mm wide slit into a vacuum chamber pumped to 2.5 Torr, a pressure that maximized the resulting signal strength. Approximately 150 mW of tunable radiation from a continuous-wave Ti:sapphire ring laser (Coherent 899-29) was mechanically chopped and multi-passed a total of four times through the gas flow, using a pair of mirrors located outside the chamber. Laser-induced fluorescence was collected at $f/2$ with a 50-mm diameter lens, passed through a colored glass filter (Schott RG9), and focused onto a side-on photomultiplier tube (Hamamatsu R-928). The choice of filter was made to optimize the signal-to-noise ratio by passing D–X (0,1) fluorescence but blocking laser scatter and short-wavelength emission from the argon discharge. The LIF signal was demodulated with an analog lock-in amplifier (Stanford SR510) using a 0.3-s time constant. The ring laser was scanned at a rate of 0.67 cm^{-1}/min. The laser's on-board wavemeter was calibrated by recording optogalvanic atomic lines of argon with a hollow cathode discharge lamp [21], which provides an estimated absolute wavenumber uncertainty of about 0.001 cm^{-1}. The molecular linewidths were limited by Doppler broadening to ~ 500 MHz (FWHM). At one stage of the experiment, significant efforts were made

to record a sub-Doppler spectrum by the method of intermodulated fluorescence spectroscopy. This attempt proved to be fruitless, as the observed Lamb dips were too weak to permit a recording of the spectrum suitable for analysis. The likely cause of this failure is the low oscillator strength of the D–X band [8], which makes it difficult to saturate a rotational transition.

3. Analysis and results

3.1. Description and assignment of the spectrum

The red-degraded $D^2\Pi_{1/2}-X^2\Delta_{3/2}$ (0,0) band of TaO displays six rotational branches, assigned as Λ-doubled pairs of P, Q, and R branches. The observed Λ-doubling arises entirely in the upper state and is quite large: the R_{ff} branch, for example, forms a head at $J'' = 31.5$ near 14341.8 cm^{-1}, while the R_{ee} head lies nearly 20 cm^{-1} further to the blue, at $J'' = 53.5$. The sign and magnitude of the Λ-doubling produces an effective B value for the $D^2\Pi_{1/2}(e)$ parity component which is larger than that of the ground state for low values of J. Consequently, the Q_{ef} branch starts out by moving to *higher* wavenumber and forming a prominent head at 14333.982 cm^{-1}, which is over 1 cm^{-1} to the blue of its origin. The shortest wavelength feature in this head is the $F = 8 \leftarrow 8$ hyperfine component of the Q_{ef}(11.5) line. The Q_{fe} branch, conversely, behaves in the manner expected for a red-degraded band, by continually moving from its origin to longer wavelength.

Hyperfine structure arising from the $I = 7/2$ spin of the ^{181}Ta nucleus (100% abundant) is well resolved for all the lines of every branch. For lines with $J \geq I$, this structure consists of eight main hyperfine components with $\Delta F = \Delta J$, which spread out in a ~0.5-cm^{-1} wide Landé pattern. The low-J rotational lines were too weak to permit the identification of any satellite components, where $\Delta F = \Delta J \pm 1$.

The process of assigning rotational and hyperfine quantum numbers to the observed lines was straightforward, since ground state combination differences were accurately known from our previous work on the molecule [19]. However, the wide hyperfine structure and dense rotational spacing combine to produce a highly congested spectrum, particularly in the region of the R_{ff} and Q_{ef} heads. Consequently, members of these two branches could only be followed over the ranges of $J'' = 2.5-22.5$ and $J'' = 21.5-32.5$, respectively, while the other four branches were assigned over a wider range of $J'' \approx 4.5-40.5$. Our analysis was not extended beyond $J'' = 40.5$, by which point the branches have become quite weak.

Fig. 1 displays representative portions of the band. The upper trace shows the uncongested R_{ee} branch just to the blue of the R_{ff} head, where the eight-line hyperfine pattern is readily apparent. The lower trace displays a portion of the spectrum where the Q_{fe}, P_{ff}, and P_{ee} branches are extensively overlapped. At higher J these branches become less crowded. The $C^2\Delta_{3/2}-X^2\Delta_{3/2}$ (3,2) band of TaO lies in the same wavelength region, and two members of its P branch are marked in the lower trace. Fortunately, the hyperfine structure of this overlapping band is narrow and unresolved, so that the interloping singlet lines could be easily identified.

The analysis of the spectrum was begun by assigning and fitting the sparser R_{ee} and P_{ee} branches and the position of the R_{ff} head. Then, with preliminary molecular constants in hand, the wavenumbers of the other branches were predicted and added to the data set without ambiguity. No local perturbations were found anywhere in the spectrum. The vibrational numbering of the band is not in doubt. A progression of the (0,0), (1,0), and (2,0) bands was seen in both the matrix work [8] and in preliminary lower-resolution pulsed laser scans of our own recording, and in neither case was a band observed one vibrational interval to longer wavelength.

3.2. The molecular Hamiltonian and least-squares fitting

The $D^2\Pi_{1/2}-X^2\Delta_{3/2}$ spectrum was fitted with a Hamiltonian expressed in a Hund's case (c) basis, since the complementary $^2\Pi_{3/2}-{}^2\Delta_{5/2}$ transition has not been observed. For the ground state, the rotational energy levels were written in a manner consistent with all previous work on the molecule as.

$$F(J) = BJ(J+1) - DJ^2(J+1)^2 + HJ^3(J+1)^3 \quad (1)$$

For the $D^2\Pi_{1/2}$ state, additional Λ-doubling terms were added so that its rotational and parity levels are described as.

$$F(J)_f^e = T_0 + BJ(J+1) - DJ^2(J+1)^2 + HJ^3(J+1)^3$$

$$\mp\frac{1}{2}\left(J+\frac{1}{2}\right)\left[(p+2q) + D_{p+2q}J(J+1) + H_{p+2q}J^2(J+1)^2\right] \quad (2)$$

The hyperfine structure of the two states was modeled using terms describing the nuclear-spin rotation, magnetic dipole, and electric quadrupole interactions. The matrix elements of these terms for a $^2\Pi_{1/2}$ state were listed in spherical tensor form in our report on the $E^2\Pi_{1/2}-X^2\Delta_{3/2}$ transition of TaO [20], so will not be given here. However, in undertaking the present analysis of the D–X system, we discovered an error in Eq. (4) of Ref. [20]: the $\pm\sqrt{1/3}$ factor in front of the hyperfine d term should be replaced with $\pm\sqrt{1/2}$. This error was propagated in the fitting routine used in the work of Ref. [20], so that the values reported there for the d parameter of the $E^2\Pi_{1/2}$ state need to be corrected to 0.043207(54) cm^{-1} for $v = 0$ and 0.052142(59) cm^{-1} for $v = 1$. This error does not affect the discussion or conclusions of Ref. [20]. For the present work, we checked our fitted results against a simulation of the D–X spectrum using the PGOPHER program [22] and found the two to be in excellent agreement. Judging from the PGOPHER simulation, we estimate the temperature of the sample of TaO to be 330 ± 30 K.

The operator involving the Λ-doubling d parameter acts between the $\Lambda = +1/2$ and $-1/2$ wavefunctions, producing different hyperfine structures in the two $^2\Pi_{1/2}$ parity components. It is this term which dominates the observed hyperfine structure of the D–X spectrum. Its contribution to the hyperfine energy is equal in magnitude but opposite in sign for the two Λ-doublets, so that in the spectrum it determines the energy order of the various F components of a rotational transition, creating a "mirror image" hyperfine structure that is apparent in the lower trace of Fig. 1. This structure facilitates an absolute parity assignment for the upper state since a positive value for d implies a positive value for $\sin^2\theta$ in the definition $d = (3/2)g\mu_B g_N \mu_N \langle \sin^2\theta/r^3 \rangle$ [20]. With this choice of sign, the e parity levels of the upper state have their maximum F component at lowest wavenumber, while the opposite is true for the f parity levels. Furthermore, this assignment places the e parity component to be above f in the $D^2\Pi_{1/2}$ state, leading to a negative value for the lambda-doubling parameter, $p + 2q$.

Accurate values for the $X^2\Delta_{3/2}$ state parameters B, D, $h_{3/2}$, and eQq_0 were previously determined in our analysis of the B–X and C–X transitions recorded at sub-Doppler resolution [19]. In that work, the observed linewidths were about a factor of 10 narrower than those of the present Doppler-limited spectrum, resulting in more precise measurements. In addition, with less spectral congestion, the branches were tracked down to their lowest-J members, where satellite ($\Delta F \neq \Delta J$) transitions were observed, providing direct hyperfine combination differences for the ground state. For these reasons, in the present work we chose to fix the four ground state parameters at the values determined in Ref. [19]. The D–X branches are fitted to much higher J'' (40.5 versus 22.5 for B–X and C–X), however, so that an additional higher-order centrifugal distortion constant H'' is required, which was well determined in the fit. (We note that if B'' and D'' were also varied, the fit

Table 1
Molecular parameters for the $X^2\Delta_{3/2}$ and $D^2\Pi_{1/2}$ states of TaO.[a]

Parameter	$X^2\Delta_{3/2}(v=0)$	$D^2\Pi_{1/2}(v=0)$
T_v	0.0	14332.42064(28)
B	0.4019957	0.3930542(16)
D	2.882×10^{-7}	$3.157(22) \times 10^{-7}$
H	$1.686(44) \times 10^{-11}$	$1.924(91) \times 10^{-11}$
$p + 2q$	–	–0.436015(29)
D_{p+2q}	–	$9.04(64) \times 10^{-7}$
H_{p+2q}	–	$4.77(33) \times 10^{-10}$
h_Ω	0.02157	0.00573(79)
d	–	0.130126(65)
eQq_0	–0.1072	–0.05570(89)
$\Delta G_{1/2}$	1021.68[c]	949.15(20)[b]
RMSD[d]	0.0021	

[a] All values in cm^{-1}, with one standard deviation in parentheses in units of the last reported digit. Ground state parameters without a reported uncertainty were fixed at the values of Ref. [19].
[b] As determined from an estimate of the (1,1) band origin (see text).
[c] From Ref. [8].
[d] Root-mean-square deviation of the fit.

variance was only marginally smaller, and the fitted values agreed with those found in Ref. [19] at the 1σ level.) At a late stage in the least-squares fitting, additional terms were added to the Hamiltonian representing the centrifugal distortion of each of the $D^2\Pi_{1/2}$ state hyperfine parameters (h_Ω,d,eQq_0) as well as a nuclear spin–rotation parameter (c_I), but none significantly reduced the variance or were determinable at the 3σ level.

The results of the least-squares fitting are presented in Table 1. A total of 821 transitions were fitted in the data set, and a list of the observed and calculated wavenumbers is provided in the supplementary material. Due to the high spectral congestion, many hyperfine components are blended with members of other unrelated lines. If a blended line was observed to be broader than the 500-MHz width typical of unblended features, it was not included in the least-squares fit. In our experience, Doppler-limited lines recorded with our spectrometer can be measured with a wavenumber uncertainty of ±0.002 cm^{-1}. The root-mean-square deviation of the fitted lines is 0.0021 cm^{-1}, which indicates that the observed lines have been fitted to within their experimental uncertainty.

The rotational, Λ-doubling, and hyperfine constants of the $D^2\Pi_{1/2}$ state have been determined here for the first time. Cheetham and Barrow [9] reported the gas-phase band origin (ν_0) as ~ 14370 cm^{-1}, which does not agree well with our fitted value of 14332.4206(3) cm^{-1}. It is possible they listed not the origin but the R_{ee} head of their (unanalyzed) band, which our least-squares fit predicts to lie near 14,361 cm^{-1}, in better agreement with their value. The D–X transition of TaO in absorption in a neon matrix was measured at 14,395 cm^{-1} [8], and its MCD spectrum in an argon matrix lies at 14,235 cm^{-1} [10]. Gas-to-matrix wavenumber shifts on this order of magnitude are in line with what has been observed for other electronic transitions of TaO [8,9]. We note that the unassigned peak labeled "Q" in the photoelectron spectrum of the TaO^- anion [18] is likely due to the D state described here, since its reported energy of 14195 ± 500 cm^{-1} agrees well with our band origin.

Finally, we simultaneously recorded the partially overlapping (1,1) band of the D–X system, which lies about 75 cm^{-1} to the red of the (0,0) band. We chose not to pursue a rotational analysis of this hot band due to its much weaker intensity. However, the wavenumbers of its two most prominent features are 14269.540 cm^{-1} for the R_{ff} head and 14258.324 cm^{-1} for the Q_{ef} head. From the latter, the (1,1) band origin can be estimated as $\tilde{\nu}_{1,1} = 14259.886$ cm^{-1} by assuming the wavenumber difference between the head and the band origin is the same as that found for the (0,0) band, which is 1.562 cm^{-1}. (This difference depends somewhat on the change in the rotational and Λ-doubling constants upon vibrational excitation of both electronic states.) In combination with the known $X^2\Delta_{3/2}$ value of $\Delta G''_{1/2} = 1021.68(4)$ cm^{-1} [8], this assumption yields a vibrational spacing of $\Delta G'_{1/2} = 949.15$ cm^{-1} for the $D^2\Pi_{1/2}$ state. A conservative estimate of the uncertainty in this value is ±0.2 cm^{-1}.

4. Discussion and conclusions

The $X^2\Delta_r$ ground state of TaO has been shown to arise mostly from the configuration $(16\sigma)^2(8\pi)^4(4\delta)^1(17\sigma)^2(9\pi)^0$ [19]. Here, the bonding 16σ and 8π orbitals are formed via overlap of Ta 5d and O 2p orbitals, with Ta 6s also contributing to 16σ. The 17σ and (empty) 9π orbitals are their antibonding counterparts. Given the electronegativity difference, one expects these bonding orbitals to be mostly oxygen in character (which leads to a $Ta^{2+}O^{2-}$ description in the fully ionic limit) and the antibonding ones mostly tantalum. The single unpaired electron is located in the 4δ orbital, which is a nonbonding Ta 5dδ orbital.

One obvious way of forming the upper $D^2\Pi$ state is to promote the unpaired 4δ electron to the 9π orbital, producing a single $^2\Pi$ state from the resulting $(16\sigma)^2(8\pi)^4(17\sigma)^2(9\pi)^1$ configuration. We speculated on this possibility to explain the character of the $E^2\Pi$ state [20], and with our density functional theory (DFT) estimates of the Hund's case (a) hyperfine parameters a, b_F, and c, we predicted a value for the observed case (c) hyperfine parameter $h_{1/2} = a\Lambda + \left(b_F + \frac{2}{3}c\right)\Sigma = a - \frac{1}{2}b_F - \frac{1}{3}c$ to be +202 MHz if the 9π molecular orbital were a pure Ta 5dπ orbital; see Refs. [19] and [20] for details. Since the $E^2\Pi$ spectroscopic value of this hyperfine parameter is $h_{1/2} = -781$ MHz, the assignment of the E state as the $\bullet\bullet\bullet(9\pi)^1$, $^2\Pi$ state could be rejected. In the present work, we have found the value of the D state magnetic hyperfine parameter to be $h_{1/2} = 172 \pm 24$ MHz, which is nearly identical to the DFT estimate of $h_{1/2} = 202$ MHz for such a $^2\Pi$ state. However, this analysis is more suggestive than persuasive, given the simple arguments used in the single configuration limit. It also does not explain the large value of the Λ-doubling hyperfine parameter in the D state, which is $d = 3901 \pm 2$ MHz (Table 1). For a single unpaired electron, the definition of the dipolar constant is $c = (3/2)g\mu_B g_N \mu_N \langle 3\cos^2\theta - 1/r^3\rangle$, so that.

$$\frac{d}{c} = \frac{\langle \sin^2\theta \rangle}{\langle 3\cos^2\theta - 1 \rangle} = \frac{4/7}{2/7} = 2 \tag{3}$$

where the angular expectation values for a dπ electron are taken from Ref. [23]. Our DFT estimate for the parameter c in a pure Ta 5d, 9π orbital is $c = 127$ MHz [19], which would make d to be 254 MHz, a factor of 15 smaller than the observed value. More detailed *ab initio* calculations are required to fully understand the unusually large value of d and to shed light on the possible configurations of the TaO upper states.

Undertaking a similar analysis of the electric quadrupole interactions in the X and D states is more complicated, since all the valence electrons contribute to eQq_0, not just the unpaired ones. The single-electron electric quadrupole parameter for each electron i can be written as.

$$eQq_{0,i} = \frac{-e^2Q}{4\pi\varepsilon_0}\left\langle \left(3\cos^2\theta_i - 1\right) r_i^{-3} \right\rangle \tag{4}$$

where e is the elementary charge, Q is the quadrupole moment of the nucleus, and ε_0 is the electric constant. In work on the related molecule TaH, we estimated semi-empirically that a Ta 5dδ electron contributes 2280 MHz to the value of eQq_0, while a Ta 5dπ electron contributes –1140 MHz [24]. These values lead to a prediction that a 4δ → 9π promotion of an electron in TaO will decrease the value of eQq_0 by 3420 MHz in going from the ground state to the D state, if the 4δ and 9π orbitals were pure Ta 5d orbitals. From Table 1, the observed decrease in eQq_0 is 1544 MHz, which is about half the predicted value. In fact, the 4δ and 9π orbitals also have significant oxygen character, which does not contribute much to the electric quadrupole interaction at the Ta nucleus,

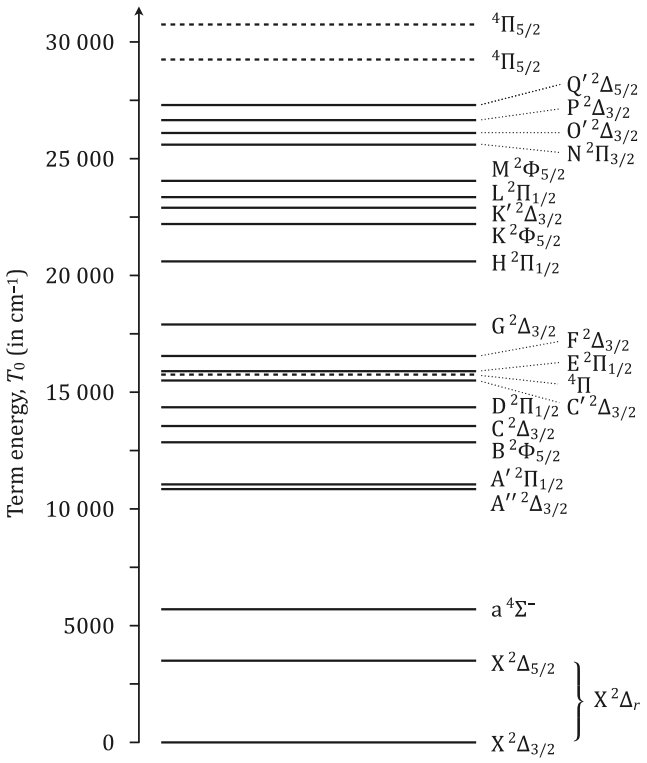

Fig. 2. Term energy map of the known electronic states of TaO. Solid lines are used for states whose absolute term energies are known. The term symbols and absolute energies of the three $^4\Pi$ states are not known with certainty. The F and G states have only been observed for TaO in a neon matrix at 4 K.

since $\langle r^{-3} \rangle$ is quite small there. Thus, mixing in O 2p character will reduce the estimate of how much eQq_0 will decrease upon electronic excitation, bringing it more in line with the observed decrease.

Since the present work represents an analysis of one of the last uncharacterized electronic states of TaO in the gas phase, it is useful to conclude by summarizing the energies of all identified states of the molecule. These are depicted in Fig. 2, which is a compilation of results from Refs. [9–13,18–20] and from the present work. Case (a) labels are used here following the tradition established in Cheetham and Barrow's first study [9], but it should be recognized that a case (c) description is more accurate, in which Ω remains a (nearly) good quantum number, but Λ does not, due to mixing with other states of different Λ by the large spin–orbit interactions in a heavy metal atom. In our work on the B, C, and E states [19,20], we could unambiguously assign values of Ω for the upper states by identifying the first lines in the three rotational branches at the relatively cold temperature of our source. In the work of other authors [9,11–13] on gas-phase TaO, the Ω' assignments are determined from the relative strengths of the P, Q, and R branches, and for $\Omega' = 1/2$ states ($^2\Pi_{1/2}$), by the presence of Λ-doubling. The MCD matrix work, where the phase of the signal reveals the value of Ω', confirmed all but one of these assignments. The value of Λ given to these upper states was then determined by the case (a) selection rule $\Delta\Lambda = \Delta\Omega$. Al-Khalili et al. [11] and Ram and Bernath [13] speculated on more than one possible (doublet or quartet) assignment for the transitions involving states marked with dashed lines in the figure. If in fact those transitions originate from a low-lying doublet state and not the $a^4\Sigma^-$ state, then the term symbols and locations of the $^4\Pi$ states shown in the figure will need to be revised.

Declaration of Competing Interest

The authors declare that they have no known competing financial interests or personal relationships that could have appeared to influence the work reported in this paper.

Data availability

Data will be made available on request.

Acknowledgements

This material is based upon work supported by the National Science Foundation under grant CHE-2100542. Kara Manke and Tyson Vervoort are acknowledged for recording and partially analyzing a preliminary spectrum of this transition several years ago. This paper is dedicated to the memory of Prof. Colin Western, with whom the corresponding author had many inspiring conversations about spectroscopy.

Appendix A. Supplementary material

Supplementary data to this article can be found online at https://doi.org/10.1016/j.jms.2022.111666.

References

[1] F. Azizi and M. T. Mirtorabi, Astrophys. Space Sci. 357 (2015) 96, https://doi.org/10.1007/s10509-015-2366-8.
[2] R.E. Schulte-Ladbeck, Astron. Astrophys. 189 (1988) 1–5.
[3] P.F. Bernath, Int. Rev. Phys. Chem. 28 (2009) 681–709, https://doi.org/10.1080/01442350903292442.
[4] A.J. Sauval, Astron. Astrophys. 62 (1978) 295–298.
[5] T. Fleig, Phys. Rev. A 95 (2017), 022504, https://doi.org/10.1103/PhysRevA.95.022504.
[6] D. Premaswarup, Nature 175 (1955) 1003, https://doi.org/10.1038/1751003b0.
[7] D. Premaswarup, R.F. Barrow, Nature 180 (1957) 602–603, https://doi.org/10.1038/180602b0.
[8] W. Weltner Jr., D. McLeod Jr., J. Chem. Phys. 42 (1965) 882–891, https://doi.org/10.1063/1.1696076.
[9] C.J. Cheetham, R.F. Barrow, Trans. Faraday Soc. 63 (1967) 1835–1845, https://doi.org/10.1039/tf9676301835.
[10] R. Brittain, D. Powell, M. Kreglewski, M. Vala, Chem. Phys. 54 (1980) 71–78, https://doi.org/10.1016/0301-0104(80)80036-X.
[11] A. Al-Khalili, U. Hällsten, O. Launila, J. Mol. Spectrosc. 198 (1999) 230–238, https://doi.org/10.1006/jmsp.1999.7953.
[12] R.S. Ram, P.F. Bernath, J. Mol. Spectrosc. 191 (1998) 125–136, https://doi.org/10.1006/jmsp.1998.7620.
[13] R.S. Ram, P.F. Bernath, J. Mol. Spectrosc. 221 (2003) 7–12, https://doi.org/10.1016/S0022-2852(03)00198-X.
[14] M. Dolg, H. Stoll, H. Preuss, R.M. Pitzer, J. Phys. Chem. 97 (1993) 5852–5859, https://doi.org/10.1021/j100124a012.
[15] F. Rakowitz, C.M. Marian, L. Seijo, U. Wahlgren, J. Chem. Phys. 110 (1999) 3678–3686, https://doi.org/10.1063/1.478257.
[16] F. Rakowitz, C.M. Marian, L. Seijo, J. Chem. Phys. 111 (1999) 10436–10443, https://doi.org/10.1063/1.480398.
[17] Z.J. Wu, Y. Kawazoe, J. Meng, Theochem 764 (2006) 123–132, https://doi.org/10.1016/j.theochem.2006.02.015.
[18] W. Zheng, X. Li, S. Eustis, K. Bowen, Chem. Phys. Lett. 460 (2008) 68–71, https://doi.org/10.1016/j.cplett.2008.06.016.
[19] K.J. Manke, T.R. Vervoort, K.T. Kuwata, T.D. Varberg, J. Chem. Phys. 128 (2008), 104302, https://doi.org/10.1063/1.2837470.
[20] C.R. Christopher, S.Y. Lee, F.B. Gwandu, A.J. Matsumoto, B.J. Knurr, T.K. Mahle, Z. W. Morrow, T.D. Varberg, J. Mol. Spectrosc. 301 (2014) 25–27, https://doi.org/10.1016/j.jms.2014.05.006.
[21] National Institute of Standards and Technology, Physical Measurement Laboratory, Atomic Spectra Database, 2022. https://physics.nist.gov/asd/, (accessed 21 April 2022).
[22] C.M. Western, J. Quant. Spectrosc. Ra. 186 (2017) 221–242, https://doi.org/10.1016/j.jqsrt.2016.04.010.
[23] T.D. Varberg, R.W. Field, A.J. Merer, J. Chem. Phys. 95 (1991) 1563–1576, https://doi.org/10.1063/1.461071.
[24] S.Y. Lee, C.R. Christopher, K.J. Manke, T.R. Vervoort, T.D. Varberg, Mol. Phys. 112 (2014) 2424–2432, https://doi.org/10.1080/00268976.2014.906676.